



Identifying the spatial drivers and scale-specific variations of soil organic carbon in tropical ecosystems: A case study from Knuckles Forest Reserve in Sri Lanka



R.P.S.K. Rajapaksha^{a,1}, S.B. Karunaratne^{b,*}, A. Biswas^c, K. Paul^d, H.M.S.P. Madawala^e, S.K. Gunathilake^f, R.R. Ratnayake^{a,*}

^a National Institute of Fundamental Studies, Hantana Road, Kandy, Sri Lanka

^b Sydney Institute of Agriculture, School of Life and Environmental Sciences, The University of Sydney, Sydney 2006, Australia

^c School of Environment Sciences, University of Guelph, Guelph, Ontario N1G2W1, Canada

^d CSIRO Land and Water, Black Mountain, Canberra, Australia

^e Department of Botany, Faculty of Science, University of Peradeniya, Peradeniya, Sri Lanka

^f Department of Natural Resources, Faculty of Applied Sciences, Sabaragamuwa University of Sri Lanka, Belihuloya, Sri Lanka

ARTICLE INFO

Keywords:

Soil carbon sequestration
Soil carbon stocks
Tropical forests
Digital soil mapping
Scale specific variation

ABSTRACT

Soil organic carbon (SOC) is a key driver of ecosystem functioning and may also contribute to climate change mitigation through the sequestration of carbon. Therefore, having an understanding of the key drivers of SOC may inform management changes that will improve ecosystem function and climate change mitigation. The selected study area is ranged from montane forests to tropical grasslands. Extensive soil sampling (0–0.15 m and 0.15–0.30 m) was undertaken across this region to inform our knowledge about key drivers of SOC at different spatial scales. Initially spatial modelling was carried out using spatial linear mixed modelling approach using a variety of environmental covariates. The model had a Lin's concordance correlation coefficient value of 56–60%, and indicated that SOC was predominately influenced by vegetation type and elevation, although the sub-surface (0.15–0.30 m) SOC was influenced by slope and wetness index. Further, four spatial transects with 100 m sampling interval were extracted from the digital maps representing the study area and empirical mode decomposition (EMD) analysis was carried out to examine the scale specific variability of SOC stocks. The EMD, a mathematical analysis, separates dominant frequencies within a spatial/temporal series representing variability created by various underlying processes operating at different scales into a finite number of scale components or intrinsic mode functions (IMFs). Decomposition of SOC spatial series for the considered transects resulted up to 7 IMFs. The scale components with lower IMF numbers separated higher frequency oscillations, whereas higher IMF numbers separated lower frequency oscillations, which is the representative of smaller and larger scale processes, respectively. Spectral analysis was performed to identify the scales of IMFs and the correlation analysis was carried out with different environmental covariates to identify the dominant controlling factors at different depths. Majority of the large-scale variations (e.g. 2037–8149 m for IMF's 6 for depth interval 0–0.15 m for transect 1–4) were attributed to the elevation and climatic factors controlling the forest type, while small-scale (e.g. 69–118 m for IMF's 1 for depth interval 0–0.15 m for transect 1–4) variations were more attributed terrain derived attributes. Similar scales were identified for the depth 0.15–0.30 m. The scale-specific controlling factors at different locations and their relative controlling factors may help in selecting environmental covariates that enables us to model SOC more accurately rather than fitting one global model. The study provided firsthand information on baseline SOC stock values from a tropical forest ecosystem with six different vegetation types. The information revealed in this study will be useful in the conservation of tropical forests in the region and towards providing vital firsthand information to establishing a national carbon accounting system for land sector in the future.

* Corresponding authors: Agriculture Victoria Research, Department of Jobs, Precincts and Regions, Ellinbank, VIC 3821, Australia.

E-mail addresses: senawusl@gmail.com (S.B. Karunaratne), renuka.ra@nifs.ac.lk (R.R. Ratnayake).

¹ Current Address: Hawkesbury Institute for the Environment, Western Sydney University, Penrith, NSW 2751, Australia.

1. Introduction

Soil organic carbon (SOC) is a key driver of ecosystem functioning (Lal, 2015) and may also contribute to climate change mitigation through the sequestration of carbon (McBratney et al., 2014; Ottoy et al., 2017; Ratnayake et al., 2017). An understanding of the key drivers of SOC is required to inform management changes that will enhance SOC stocks, and hence, ecosystem functions and for climate change mitigation (Mishra et al., 2009; Xia et al., 2010; Stockmann et al., 2013).

Quantification of baseline SOC stocks and identification of drivers in spatial domains are challenging (Karunaratne et al., 2014b). In natural systems, SOC stocks are influenced by a number of processes occurring together at different intensities and different scales. The emerging technologies of Digital Soil Mapping (DSM) together with Empirical Mode Decomposition (EMD) analysis may provide an assessment of key factors influencing SOC stocks at specific spatial scales (McBratney et al., 2003; Biswas and Si, 2011; Biswas et al., 2013), with the EMD analysis identifying unique processes as unique Intrinsic Mode Function's (IMF) (Huang et al., 2015). Such methodologies may facilitate efficient monitoring of management-induced changes to baseline stocks (Zhu et al., 2017).

While there are many research outputs on global scale modelling and mapping of SOC (e.g. Hengl et al., 2014; Viscarra Rossel et al., 2014; Stockmann et al., 2015), only limited number of work is available on detailed analysis of SOC and the factors that influence C in tropical forest soil (Clark, 2004; Houghton, 2005). Research reported so far recorded that the labile C pools are primarily influenced by inputs of organic matter such as plants and animals, which contribute significantly to nutrient cycling (Bolton et al., 1993; Hoyle et al., 2008; Kölbl et al., 2014; Ratnayake et al., 2017). The alteration of native vegetation causes a reduction in surface total organic carbon stocks mainly through a reduction in the quantity of plant inputs into the soil, increasing erosion rates, and an acceleration of the decomposition of soil organic matter (Assis et al., 2010; Sousa et al., 2012; Albaladejo et al., 2013). The different types of vegetation, which are in different climate, soil and landscape conditions, have also found to affect SOC content of forest soils (Fissore et al., 2008). The quantity and quality of SOC decreased with increasing mean annual temperatures because, temperature sensitivity values were strongly and positively related to SOC decomposition rates (Fissore et al., 2008). The natural disturbances such as wind, fire, drought, insects and diseases can cause changes in soil moisture, temperature regimes and succession of forest species with differences in quantity and quality of biomass returned to the soil (Overby et al., 2003; Lal, 2005; Scheller et al., 2011). These natural disturbances (e.g. fire) may also change the canopy cover, and thereby affect soil erosion (Elliot, 2003), which also affects SOC content in the surface layer.

The terrestrial C pool has been greatly reduced by human activities such as conversion of forests into agricultural land and urban areas (Jandi et al., 2007). This has been a major issue in the tropics in comparison to other regions and thereby leads to take actions for the conservation and management of these valuable tropical forest ecosystems (Gupta and Sharma, 2011; Jeyanny et al., 2014; Tanner et al., 2016).

The overall objective of this study was to characterize and quantify the scale-specific spatial variability of SOC stocks in tropical ecosystems and identify their dominant controls. The study was carried out in Knuckles Forest Reserve (KFR) in Sri Lanka. The specific objectives were to; (i) identify the key environmental drivers and then use them to develop a spatial prediction function to model and map SOC stocks at two different depth intervals across the landscapes using spatial linear mixed models (LMM) (ii) quantify the scale-specific variability of SOC stocks using EMD analysis, and (iii) identify the dominant controls of SOC stock variability at different scales. Although KFR inherits majority of the area still covered by primary forest types, but some parts of the

forested area are degraded due to anthropogenic activities. Therefore, it is vital to identify how the belowground SOC stocks change with these different vegetation types in KFR. We hypothesized that different vegetation types and different environmental covariates will drive SOC stocks at different spatial scales. We deployed a novel approach to test our hypothesis where initially high spatial resolution digital maps of SOC stocks were derived using spatial LMM and subsequently EMD was carried out on linear transect extracted from the digital maps to assess detailed scale-specific variation.

2. Materials and methods

2.1. Study area

The detailed analysis of SOC was carried out in an area of highly ecologically importance, KFR (Bambaradeniya and Ekanayake, 2003), a tropical forest ecosystem located in the central massif of Sri Lanka. The climatic conditions such as precipitation, wind, temperature are highly heterogeneous in KFR. South-western and North-eastern monsoonal rains directly influence the distribution of rainfall resulting a climatic variation within the KFR as it is located almost perpendicular to the direction of the respective wind currents (de Rosayro, 1958; Legg, 1995; Werner, 1982). This diverse climatic condition coupled with a rugged terrain provides a good case study region with diverse types of vegetation that can be considered as main drivers of SOC. The KFR (7°17' to 7°21'N and 80°49' to 80°57'E) covers approximately 21,000 ha of upland and highland penneplains of Sri Lanka (Fig. 1a). The major vegetation types are montane forests (MF), sub montane forests (SM), moist monsoon forests (MM), open and sparse forests (OS), grasslands (GL) and forest plantations (FP) (Bambaradeniya and Ekanayake, 2003) (Fig. 1b). The area has two main soil groups: Reddish Brown Earth (Word reference base Major group: Luvisols) and Red - Yellow Podzolic soils (Word reference base Major group: Acrisols) (Panabokke, 1996, IUSS Working Group WRB, 2015).

2.2. Soil sampling and laboratory analysis

A stratified random sampling scheme was adapted to collect soil samples using a soil core (5 cm diameter), with vegetation types as strata. Consistent with guidelines prepared by Food and Agriculture Organization (FAO) to share national datasets to compile Global Soil Organic Carbon (GSOC) Map, the soil samples were collected from 0–0.30 m, including 0–0.15 m and 0.15–0.30 m depth intervals (FAO, 2017). The litter layer was removed from the soil surface prior to collect the soil sample using the soil core. Following the approach of Dorji et al. (2014) and Karunaratne et al. (2014a), small-scale variations across each stratum were accounted by sampling an additional sample approximately distance of 1000 m. In total of 190 sites of soil sampling locations were included in the current study, spatially distributed across the study area (Table 1). At each sampling site, GPS locations were recorded using a Garmin eTrex 30 handheld GPS receiver.

In laboratory, first soil samples were air dried and sieved using a 2 mm mesh sieve after removing all visible organic debris, stones and plant roots. Prior to SOC analysis, the sieved soil samples were ground, and 1 ± 0.001 g of ground soil sample was used for the analysis. The SOC contents were determined using 'wet' oxidation by acidified dichromate of organic carbon (Baker, 1976). The bulk density of the soil samples were determined using the approach outlined in Blake and Hartge (1982). In summary, bulk density of soil was determined by the core method. The samples for bulk density were drawn after removing surface litter layer. The soil cores collected from each site were dried in an oven at 105 °C for 2 days. Bulk density was calculated as the ratio of dry mass of soil core and internal volume of the metallic core (Eq. (1)).

$$\text{Soil Bulk Density (g cm}^{-3}\text{)} = \frac{\text{Dry mass of soil (g)}}{\text{Core volume (cm}^3\text{)}} \quad (1)$$

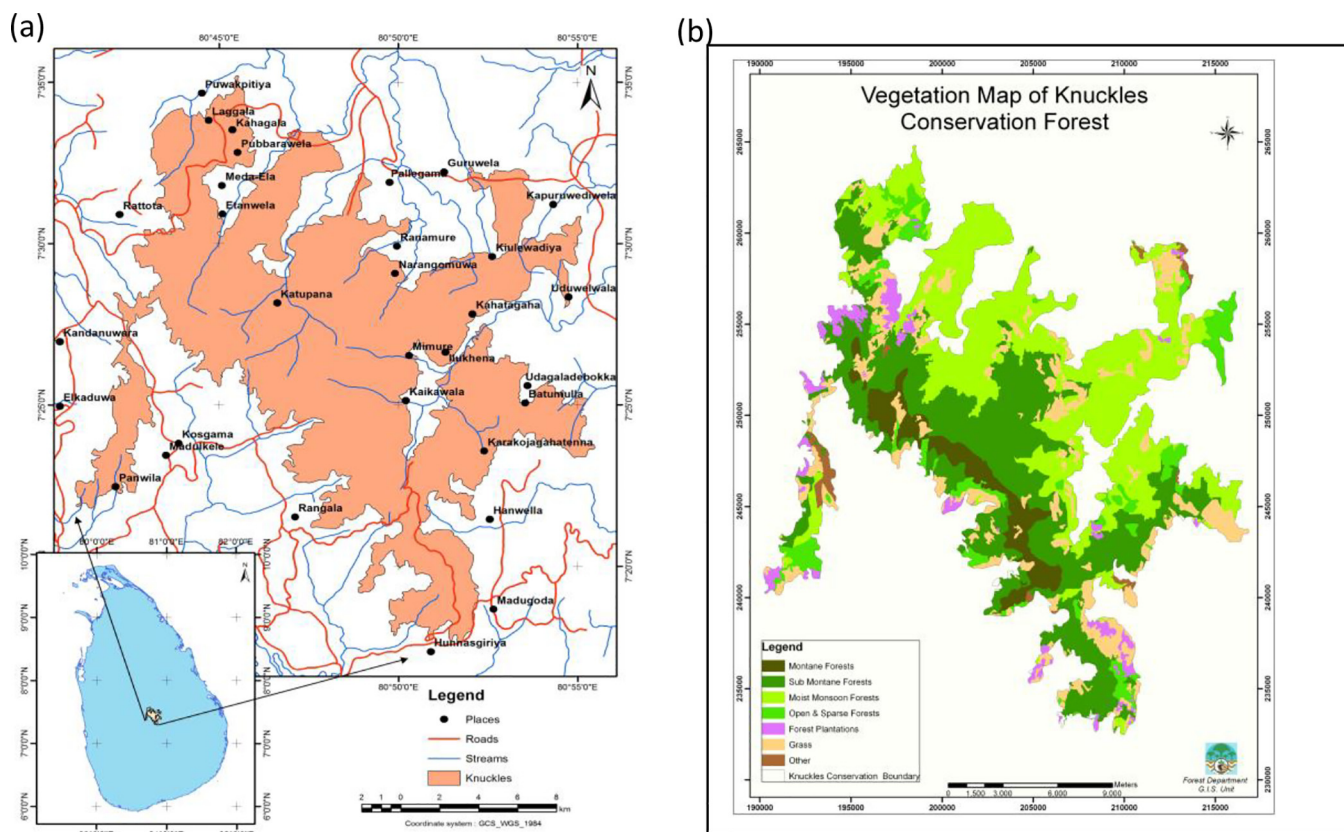


Fig. 1. The Knuckles Forest Reserve in Sri Lanka. (a) The location map. (b) Major vegetation types (Note: FP-Forest Plantations, GL-Grasslands, MF-Montane Forests, MMF-Moist Monsoon Forests, OSF-Open and Sparse Forests, SMF-Sub Montane Forests) and its distribution within the Knuckles Forest Reserve (Coordinate System: Sri Lankan National Grid; Source: Forest Department, 2007).

Table 1

Distribution of soil sampling locations across the major vegetation groups in the Knuckles Forest Reserve.

Forest type	Depth 0–0.15 m	Depth 0.15–0.30 m	Total
FP	12	11	23
GL	38	39	77
MF	14	14	28
MMF	49	49	98
OSF	27	27	54
SMF	50	50	100

Key: FP-Forest Plantations, GL-Grasslands, MF-Montane Forests, MMF-Moist Monsoon Forests, OSF-Open and Sparse Forests, SMF-Sub Montane Forests.

Finally, SOC stocks were calculated as below (Benbi et al., 2015) (Eq. (2));

$$\text{SOC Stock (C Mg ha}^{-1}\text{)} = \text{C content (\%)} \times \text{Bulk Density (Mg m}^{-3}\text{)} \times \text{Depth (m)} \times 100 \quad (2)$$

2.3. Mapping spatial distribution of SOC stocks

2.3.1. Spatial modelling and mapping framework

The SOC stocks at each depth interval were first modelled and mapped using spatial LMM. The general form of LMM applied was as below (Karunaratne et al., 2014a,b; Lark et al., 2006; Ratnayake et al., 2016) (Eq. (3));

$$\mathbf{z} = \mathbf{X}\boldsymbol{\tau} + \mathbf{Z}\mathbf{u} + \boldsymbol{\varepsilon} \quad (3)$$

where \mathbf{z} is a vector of observed n observations (SOC stock C Mg ha⁻¹), \mathbf{X} is an $n \times p$ design matrix that associates each of the SOC observations with a value of each p environmental covariates/fixed effect terms (see

Table 2 and parsimonious model is selected as described below), and $\boldsymbol{\tau}$ is a vector that contains the p fixed effect terms coefficients. The vector \mathbf{u} contains q random effect terms, realisations of a variable u , that are associated with the n observations by the $n \times q$ design matrix \mathbf{Z} . The u is spatially dependent random variable and the term $\boldsymbol{\varepsilon}$ is a vector of independent random errors.

2.3.2. Preparation of the environmental covariates

Environmental covariates were used to represent \mathbf{X} design matrix, Eq. (3). These environmental covariates represented the different elements of the *scorpan* model as the general soil spatial prediction model (McBratney et al., 2003) (Table 2). The *scorpan* model represents quantitative relationships between SOC stocks and environmental covariates within the spatial soil prediction function. It is an extension to well-known five factors of soil formation outlined by Jenny (1994).

All data sources (Table 2) were converted into 100 m spatial resolution. The DEM, slope and wetness index datasets were resampled into 100 m spatial resolution using nearest neighbor technique. All climatic variables and mean EVI data were extracted to a common grid considering its original spatial resolution and then fitted a spline model in order to re-interpolate into a grid of 100 m spatial resolution. This approach was adapted due to the artifact that resulted in predicted SOC maps when these environmental covariates were resampled to 100 m spatial resolution using nearest neighbor technique from lower spatial resolution data to higher spatial resolution. The spline interpolation was carried out using ArcGIS Version 10.2 (ESRI, 2011) using the spline toolbox with the default settings.

2.3.3. Model fitting and mapping

Initially, all the environmental covariates (Table 2) were included in the LMM. Then the most parsimonious spatial LMM model was selected

Table 2

Summary of the environmental covariates included in the development of spatial prediction function using spatial linear mixed modelling framework.

Name	Units	Original resolution/scale	Component represents the <i>scorpan</i> model	Source/Reference
Digital Elevation Model (DEM)	M	~90 m	R	NASA SRTM data http://www.cgiar-csi.org/data/srtm-90m-digital-elevation-database-v4-1
Slope	Degrees	~90	R	Derived from NASA STRM (primary terrain attribute)
Wetness index (WI)	Unit less	~90 m	R	Derived from NASA STRM (secondary terrain attribute)
Mean annual cumulative rainfall	mm	1000 m	C	Worldclim http://www.worldclim.org/
Mean annual temperature	°C	1000 m	C	Worldclim http://www.worldclim.org
Mean Enhanced Vegetation Index (EVI)	Unit less	500 m	O	NASA https://modis.gsfc.nasa.gov/data/dataproduct/mod13.php . Derived from taking mean annual EVI data from 2005 to 2014.
Forest type map	Unit less	1 cm = 2250 m	O	Forest Department, Sri Lanka, 2007

Key: R – Relief, C – Climate, O – Organisms.

using backward elimination based on Wald tests through iterative model fitting process (Karunaratne et al., 2014a,b), ensuring that $p \leq 0.10$ at a confidence interval of 90%. Prediction of SOC across the landscapes were carried out using empirical best linear unbiased prediction (E-BLUP, Karunaratne et al., 2014a,b). Entire analysis was carried out using customise R code using geoR (Diggle and Ribeiro, 2007) and gstat (Pebesma, 2004) R packages.

2.3.4. Model quality assessment

Model quality was assessed using leave-one-outcross-validation where each observation was removed from the data set and the SOC stock at that location was predicted using the remaining observations. Four measures of model quality were calculated:

Mean error (ME)

$$ME = \frac{1}{n} \sum_{i=1}^n (y_i - \hat{y}_i) \quad (4)$$

where y_i is the measured SOC stock while \hat{y}_i is the predicted SOC stock from leave-one-outcross-validation.

Root mean square error (RMSE)

$$RMSE = \sqrt{\frac{1}{n} \sum_{i=1}^n (y_i - \hat{y}_i)^2} \quad (5)$$

Mean standardized squared deviation ratio (MSDR)

$$MSDR = \frac{1}{n} \sum_{i=1}^n \frac{(y_i - \hat{y}_i)^2}{\sigma_i^2} \quad (6)$$

where σ_i^2 is the prediction variance from E-BLUP.

Lin's concordance correlation coefficient (CCC)

$$\rho_c = \frac{2\rho\sigma_x\sigma_y}{\sigma_x^2 + \sigma_y^2 + (\mu_x - \mu_y)^2} \quad (7)$$

where; ρ_c is the estimated CCC, μ_x and μ_y are the means for the measured and predicted SOC stocks and σ_x^2 and σ_y^2 are the corresponding variances of measured and predicted SOC stocks and ρ is the Pearson correlation coefficient between the measured and predicted SOC stocks.

2.4. Evaluation of soil organic carbon stock among the vegetation types

Additional analysis was performed to evaluate the SOC stock among the vegetation types. This analysis is aimed at assessing whether SOC stocks differ among the vegetation types. For this an ANOVA was performed using linear mixed model. The linear mixed model was fitted

considering vegetation type as a fixed effect term and location as a random effect term. Parameters of the linear mixed model were estimated using Restricted Maximum likelihood (REML). Here two separate linear mixed models were fitted considering two depth intervals considered in the current study. In order to assess the statistical significance of SOC stocks among the vegetation type, mean separation was carried out using least square means method (considering 0.05 probability level). Data were modelled using R statistical programming environment using nlme R package (Pinheiro et al., 2019).

2.5. Analysis of scale specific variation

A total of four transects were derived representing the different direction of the study area with sampling distance of 100 m (Appendix, Fig. A.1). Transect 1 runs from north-west to south-east with total distance of 30.1 km. Other three transects runs from south-west to north-east directions and almost parallel to each other and reported distance of 10.6 km, 17 km, 12.9 km for transect 2, 3, and 4, respectively. The directions were set based on the major directions of variability accommodating the longest distance. Predicted SOC stock (for two depth intervals) using spatial LMM and corresponding environmental covariates at those locations were extracted along the transects.

Extracted SOC stock values along the transects were then decomposed using the noise-assisted EMD (Biswas and Si, 2011). The variability of natural systems including SOC stocks are controlled by a number of processes occurring together at different intensities and scales. The EMD analysis was used to differentiate processes with similar scales as mode functions commonly known as IMF (Biswas and Si, 2011) (Eq. (8)):

$$Y(x) = \sum_{j=1}^n C_j(x) + r_n(x) \quad (8)$$

where $Y(x)$ is function of distance x , C_j is function of space and $r_n(x)$ = residuals.

Measured soil properties represent the variations of underlying soil processes. Multiple processes operating in different intensities and scales can be reflected in the spatial series as multiple oscillations. The EMD analysis can separate the influence of these individual processes into multiple IMFs and decompose the overall variability. These IMFs are generally extracted through a shifting processes after identifying local maxima, minima and their average. The average is then subtracted from the original spatial series. If the difference satisfies a set of conditions, it can be considered as IMF and will separate the highest frequency or smallest scale variations (Huang et al., 1998). This process is then repeated until it does not satisfy the conditions to be an IMF. After separating all the IMFs, the residuals generally show the overall trend and presented by a monotonic function. Here the residual represented the underlying trend in the SOC stocks over the study area. To identify

the scales of derived IMFs associated with each transect, periodogram analysis was conducted. The scales of the IMFs were determined using power spectral density analysis and the global maxima of the periodogram.

Additionally, number of analyses were performed to evaluate the scale specific contribution of separated IMFs associated with each transect. The variance associated with each IMF represents the contribution of that particular scale processes towards the overall variability Eq. (9);

$$\text{IMF Contribution Percentage} = \frac{\text{Variance of an IMF} \times 100}{\sum_{i=1}^n \text{IMF} + \text{Residuals}} \quad (9)$$

Therefore, the total variation of the spatial series of SOC stocks for the respective transects can be calculated as sum of variation of IMFs and residuals. Once the IMF were derived, correlation analysis was performed with SOC stocks and environmental covariates to identify how they are correlated with the different IMFs. In this analysis the vegetation type covariate was excluded from the analysis as it is a categorical variable. Detailed theory associated with the EMD analysis and subsequent analysis followed on this manuscript can be found in Biswas and Si (2011) and Biswas et al. (2013) and explanation of theoretical aspects are beyond the scope of this paper. The EMD analysis was performed using MATLAB software (MathSoft Inc., 2013) as explained by Biswas and Si (2011) and Biswas et al. (2013).

3. Results

3.1. Summary statistics for soil carbon stocks

The mean SOC stock for the study area was 30.3 Mg ha⁻¹, 24.3 Mg ha⁻¹ for 0–0.15 m and 0.15–0.30 m depths, respectively. Among the different vegetation groups, the lowest mean SOC stocks was in FP (23.9 Mg ha⁻¹) while the highest was in MF (39.1 Mg ha⁻¹) within top 0–0.15 m depth (Table 3). Soil organic carbon stocks in SMF, MMF, OSF and GL within 0–0.15 m depth were 36.0, 28.0, 27.1 and 27.0 Mg ha⁻¹, respectively (Table 3). The distributions for SOC stocks for considered vegetation types are depicted in the Fig. 2. For all the considered vegetation types, the mean SOC stocks reported for 0–0.15 m were higher than the 0.15–0.30 m depth interval sampling (Fig. 2/Table 3).

Table 3 summarises the estimated mean SOC values, and lower and upper confidence intervals at 0.05 probability level. If the calculated confidence intervals for respective vegetation types were overlapped each other, then it was considered that estimated mean SOC stock

Table 3

The mean separation results among the vegetation types for two depth intervals.

Model	Vegetation type [#]	Mean SOC (Mg ha ⁻¹)	Lower confidence interval (Mg ha ⁻¹)	Upper confidence interval (Mg ha ⁻¹)
0–0.15 m	FP	23.9	19.3	28.5
	GL	27.0	24.4	29.6
	MF	39.1	34.9	43.4
	MMF	28.0	25.8	30.3
	OSF	27.1	24.0	30.1
	SMF	36.0	33.8	38.3
0.15–0.30 m	FP	16.6	11.2	22.0
	GL	21.1	18.2	24.0
	MF	34.5	29.7	39.3
	MMF	21.4	18.8	24.0
	OSF	23.0	19.5	26.5
	SMF	29.0	26.5	31.6

[#] Vegetation type: Forest Plantations (FP), Grasslands (GL), Montane Forests (MF), Moist Monsoon Forests (MMF), Open and Sparse Forests (OSF), Sub Montane Forests (SMF).

values were not statistically different at considered probability level ($p < 0.05$) and vice versa (Table 3). The mean SOC stock reported in FP was significantly different from SOC stocks reported in forest types namely MF and SMF for both depth intervals (Table 3). Similarly, the mean SOC stock for GL was significantly different from the MF and SMF for both depth intervals. In terms of mean SOC stock for MF, it was significantly different from MMF and OSF for depth interval 0–0.15 m. The mean SOC stock in MMF, was significantly different from the mean SOC stock reported in SMF for depth interval 0–0.15 m.

3.2. Spatial drivers of SOC stocks in Knuckles forest reserve and model quality assessment

Two independent spatial LMMs were fitted to quantify the spatial drivers and spatial auto-correlation for residuals *i.e.* unexplained variability of SOC stocks by the environmental covariates. Summary of the estimated fixed effects and random effects are depicted in the Table 4 and Table 5 respectively.

3.2.1. Spatial drivers of SOC stocks in Knuckles forest reserve: Fixed effect terms identified by spatial linear mixed models

Vegetation type and DEM were identified as the predominantly drivers of SOC stocks for two depth intervals (Table 4). For the lower depth layer, slope and WI were also identified as statistically significant ($p < 0.10$) spatial drivers of SOC stocks. The elevation of the study area varied between 300 m and 1900 m which resulted micro-climatic conditions and was found to be a common driver for SOC stocks for two depth intervals considered in this study.

3.2.2. Spatial drivers of SOC stocks: Random effect terms identified by spatial linear mixed models

The estimated random effect terms for the spatially correlated errors are depicted in the Table 5. These residuals represent the unexplained variability by the fixed effect terms (included in the Table 4) associated with the respective depth interval models. The nugget/sill ratio was 53% and 57%, indicating fitted models consisted of moderate spatial structure (Cambardella et al., 1994). Cambardella et al. (1994) categorized spatial dependence based on variogram parameters namely on the nugget/sill ratio as; high (0–25%), moderate (25–75%) and low (> 75%). It was reported that the spherical model correlation structure was selected that the optimum model to explain the random effect terms included in the spatial LMM for the two considered depth intervals. Residuals were spatially correlated up to 4000 m and 3374 m for 0–0.15 m and 0.15–0.30 m sampling depth intervals respectively.

3.2.3. Validation of derived spatial models

Model prediction capabilities decreased at the lower depth where CCC value was reported as 0.56 while 0.60 for upper depth interval (Table 6). This is common in many DSM projects since environmental covariates derived from remotely sensed datasets are most explained the upper earth surface information rather below surface information (Bishop et al., 2015). The MSDR value for both models reported value closer to one (1) which indicated that the residuals were properly modelled. With regard to the model accuracy (RMSE), higher accuracy was reported for the 0–0.15 m model (6.93 C Mg ha⁻¹) compared to 0.15–0.30 m model (7.93 C Mg ha⁻¹) (Table 6). Lower model bias (ME) was reported for the 0.15–0.30 m model.

Despite modelling and mapping is carried out using two depth intervals similar spatial pattern has been reported for SOC (Fig. 3). The distribution of the SOC stocks for both sampling depth intervals follows the same pattern. Based on the maps, it is clearly evident the influence of the DEM on SOC stocks. As per the maps, higher elevations reported accumulation of higher SOC stocks while low lying areas represent less SOC stocks. As reflected in the derived maps, the variation of the SOC across the study area also associated with the vegetation type (see Fig. 1b for vegetation types).

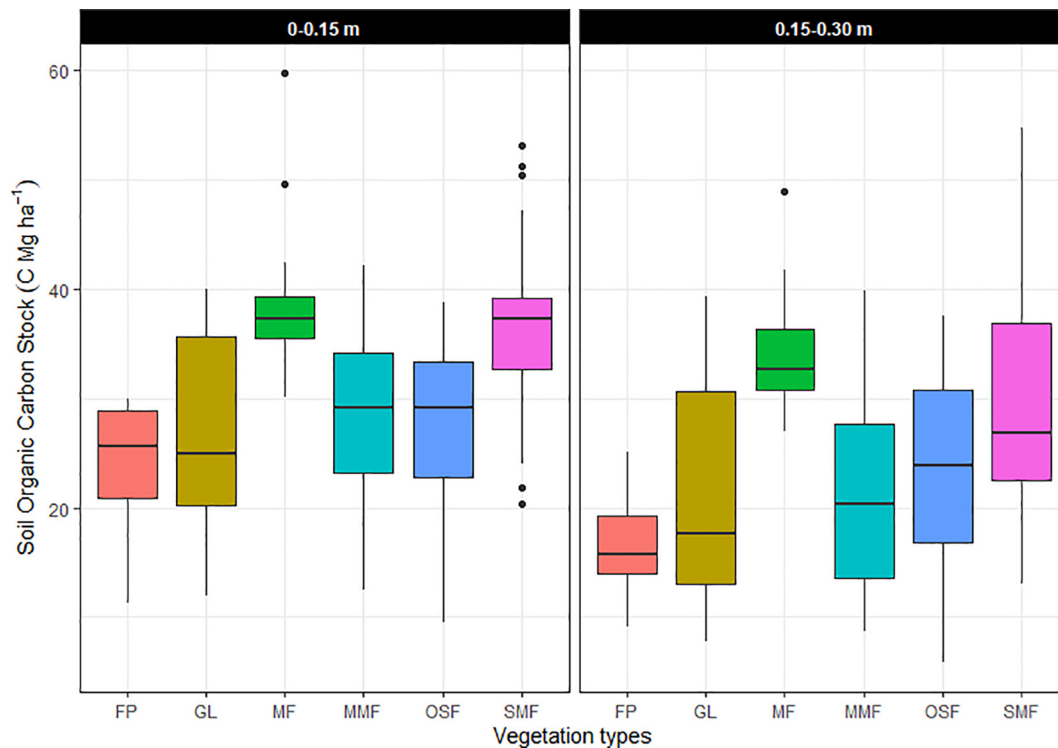


Fig. 2. Distribution of soil organic carbon stocks under different vegetation types. Grasslands (GL), Montane Forests (MF), Moist Monsoon Forests (MMF), Sub Montane Forests (SMF), Open and Sparse Forests (OSF), Forest Plantations (FP). In these boxplots mean SOC values are depicted in solid horizontal line while whiskers represent the inter-quartile range and outliers are depicted as ‘dots’ for each vegetation type.

Table 4
Major drivers of soil organic carbon in Knuckles forest reserve.

Model	Name of the coefficient	Estimated coefficients	Standard error	t-value	Probability
Depth 0–0.15 m	Intercept	$1.51 * 10^{+01}$	$3.65 * 10^{+00}$	$4.13 * 10^{+00}$	$5.572 * 10^{-05***}$
	GL	$1.76 * 10^{-01}$	$2.26 * 10^{+00}$	$7.80 * 10^{-02}$	0.938
	MF	$8.76 * 10^{+00}$	$3.19 * 10^{+00}$	$2.74 * 10^{+00}$	0.007**
	MMF	$4.37 * 10^{+00}$	$2.58 * 10^{+00}$	$1.69 * 10^{+00}$	0.092
	OSF	$-5.03 * 10^{-01}$	$2.51 * 10^{+00}$	$-2.01 * 10^{-01}$	0.841
	SMF	$6.82 * 10^{+00}$	$2.35 * 10^{+00}$	$2.89 * 10^{+00}$	0.004**
	DEM	$1.00 * 10^{-02}$	$2.93 * 10^{-03}$	$3.44 * 10^{+00}$	0.001***
	Depth 0.15–0.30 m	Intercept	$-5.75 * 10^{+00}$	$6.32 * 10^{+00}$	$-9.11 * 10^{-01}$
GL	$1.08 * 10^{+00}$	$2.66 * 10^{+00}$	$4.05 * 10^{-01}$	0.686	
MF	$9.31 * 10^{+00}$	$3.73 * 10^{+00}$	$2.50 * 10^{+00}$	0.013*	
MMF	$6.41 * 10^{+00}$	$3.01 * 10^{+00}$	$2.13 * 10^{+00}$	0.035*	
OSF	$1.19 * 10^{+00}$	$2.98 * 10^{+00}$	$3.98 * 10^{-01}$	0.691	
SMF	$6.53 * 10^{+00}$	$2.77 * 10^{+00}$	$2.36 * 10^{+00}$	0.020	
DEM	$1.38 * 10^{-02}$	$3.31 * 10^{-03}$	$4.16 * 10^{+00}$	$4.967 * 10^{-05***}$	
Slope	$1.74 * 10^{-01}$	$7.30 * 10^{-02}$	$2.39 * 10^{+00}$	0.018*	
WI	$1.03 * 10^{+00}$	$4.60 * 10^{-01}$	$2.25 * 10^{+00}$	0.026*	

Level of significance: 0 ‘***’ 0.001 ‘**’ 0.01 ‘*’ 0.05 ‘.’ 0.1.

Table 5
Estimated random effect terms for the spatially correlated errors obtained from spatial LMM.

Model	Nugget (C Mg ha ⁻¹) ²	Partial Sill (C Mg ha ⁻¹) ²	Range (m)	Nugget/Sill * 100 [#] (%)
0–0.15 m model	32.53	28.72	4000	53
0.15–0.30 m model	43.11	32.35	3374	57

[#] Sill = Nugget + Partial Sill.

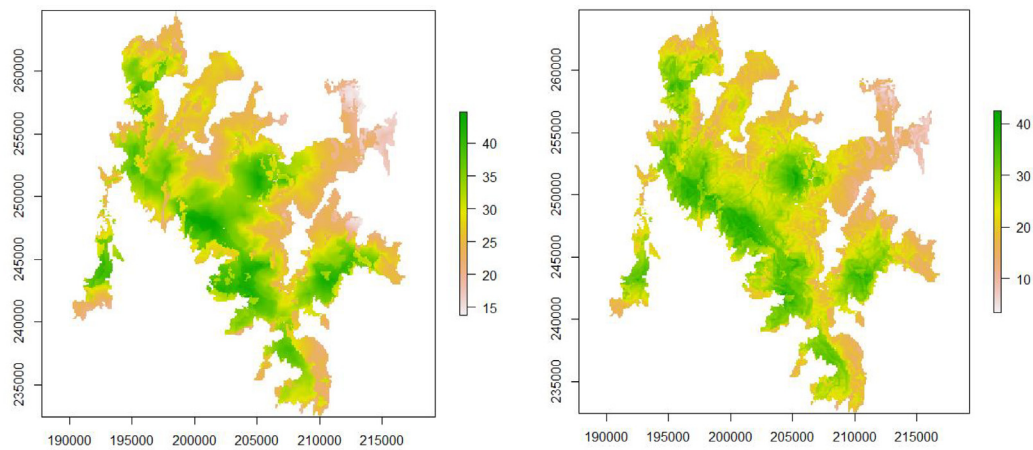
3.3. Scale specific spatial variability and their dominant controls

Decomposition of SOC spatial series for the considered transects resulted up to 7 IMFs (Appendix, Fig. A.2). Then the dominant scales for

Table 6
Model quality indices derived from the leave-one-out cross-validation.

Model	ME (C Mg ha ⁻¹)	RMSE (C Mg ha ⁻¹)	MSDR	CCC
0–0.15 m model	0.10	6.93	1.00	0.60 (0.52–0.68)
0.15–0.30 m model	0.07	7.93	0.99	0.56 (0.47–0.64)

these IMF’s were identified through spectral analysis and summarised in Table 7. The graphical summary of the scale analysis for transect 1 is depicted in Fig. 4 as per the corresponding depth intervals. The enlarged section of the Fig. 4 provides details of the variation at small scales. The scale components with lower IMF numbers separated higher frequency oscillations, whereas higher IMF numbers separated lower



a) Soil organic carbon distribution 0–0.15 m

b) Soil organic carbon distribution 0.15–0.30 m

Fig. 3. Spatial distribution of soil organic carbon stocks in Knuckles forest reserve. The SOC stocks are expressed as C Mg ha⁻¹.

Table 7

Scales (m) of IMFs determined from power spectral density analysis.

	Transect 1		Transect 2		Transect 3		Transect 4	
	0–0.15 m	0.15–0.30 m						
IMF1	79	64	118	104	77	77	69	72
IMF2	204	204	263	177	160	177	204	181
IMF3	204	243	407	263	263	263	326	240
IMF4	362	494	543	479	429	407	479	509
IMF5	1164	1254	1630	1164	1164	1019	1358	1358
IMF6	2037	2037	8149	2716	2716	2037	8149	2716
IMF7	16,297	5432						
Residuals	16,297	16,297	8149	8149	8149	8149	8149	8149

frequency oscillations, which is the representative of smaller and larger scale processes, respectively (Biswas et al., 2013). The residuals represented the overall trend in SOC stock variation along the transects for considered depth intervals. Scale interval of 69–118 m reported for IMF's 1 while 2037–8149 m for IMF's 6, respectively for depth interval 0–0.15 m for transect 1–4. Similar scales were identified for the depth interval 0.15–0.30 m for transect 1–4. Residuals for the decomposed SOC stock spatial series reported a scale value up to 16,297 m for two depth intervals for transect 1 (Table 7). Other three transects reported a scale value of ~8000 m for considered two depth intervals.

The summary of the variation explained by the extracted IMFs for each transect and depth interval together with the variation explained by residual are summarised in the Table 8. Results revealed that the variation explained by the IMFs for respective depth intervals explains ~60% of the total variation except for transect 2 depth interval 0.15–0.30 m and associated both depth intervals for transect 3 (Table 8). It should be noted that variation explained by decompose SOC stock signal (*i.e.* IMFs) and overall trend (through residuals) varies among the transects and considered depth intervals.

The correlation plot for the IMF's, residuals and environmental covariates for transect 1 depth intervals 0–0.15 m and 0.15–0.30 m is given in the Fig. 5 while for other transects are included under the Appendix, Fig. A.3. The correlation pattern for the two depth intervals for the transect 1 followed the same pattern (Fig. 5). The correlation analysis revealed that at large spatial scales, temperature, rainfall, EVI, DEM, slope and WI showed either positive or negative correlation with the IMFs 5, 6, 7. In contrast, for small spatial scales, DEM derived covariates showed some correlation among the IMFs 1, 2, 3 and 4 (Fig. 5).

4. Discussion

Several previous estimations of SOC stocks on different land cover types at global and regional scales are summarized in Table 9 and compared with the current study estimates. In the current study, the mean SOC stock of MF (39.10 Mg ha⁻¹) at a soil depth of 0–0.15 m in KFR was relatively higher than tropical montane forests in West Malaysia (Jeyanny et al., 2014) for the same depth level and the SOC stock within upper 0–0.10 m soil layer in tropical montane forests in Costa Rica (Tanner et al., 2016). The primary forests of Singapore also recorded relatively lower SOC stock (34.3 Mg ha⁻¹) even within 0–0.20 m depth interval (Ngo et al., 2013) compared to upper soil layer (0–0.15 m) of MF (39.10 Mg ha⁻¹) in KFR. Both evergreen forests and deciduous forests in the tropical region reported relatively higher SOC stocks for upper 0.30 m depths (Toriyama et al., 2011) compared to MMF in the current study (Table 9). Soil organic carbon stock in MMF was closely related with the open forests in Kashmir (Shaheen et al., 2017). Similarly, carbon stocks in OSF soil were in accordance with the open forests in Kashmir, while relatively higher than their disturbed forests as reported by Shaheen et al. (2017). Soils under the GL in KFR showed a relatively lower SOC stock within 0–0.15 m soil depth than the SOC stock value in tropical Sparse shrub/Herbaceous within 0–0.30 m soil depth according to the study of Petri et al. (2010).

Plant residues are the major source of organic carbon inputs into SOC. The quality and quantity of these residues will vary with vegetation types (Ratnayake et al., 2017). It is therefore to be expected that vegetation type was a key factor influencing SOC stocks (Table 4). For example, the relatively low SOC stocks associated with FP vegetation may have been attributable to the relatively low decomposability of pine needles (e.g. Edmonds, 1991). Vegetation type may have also

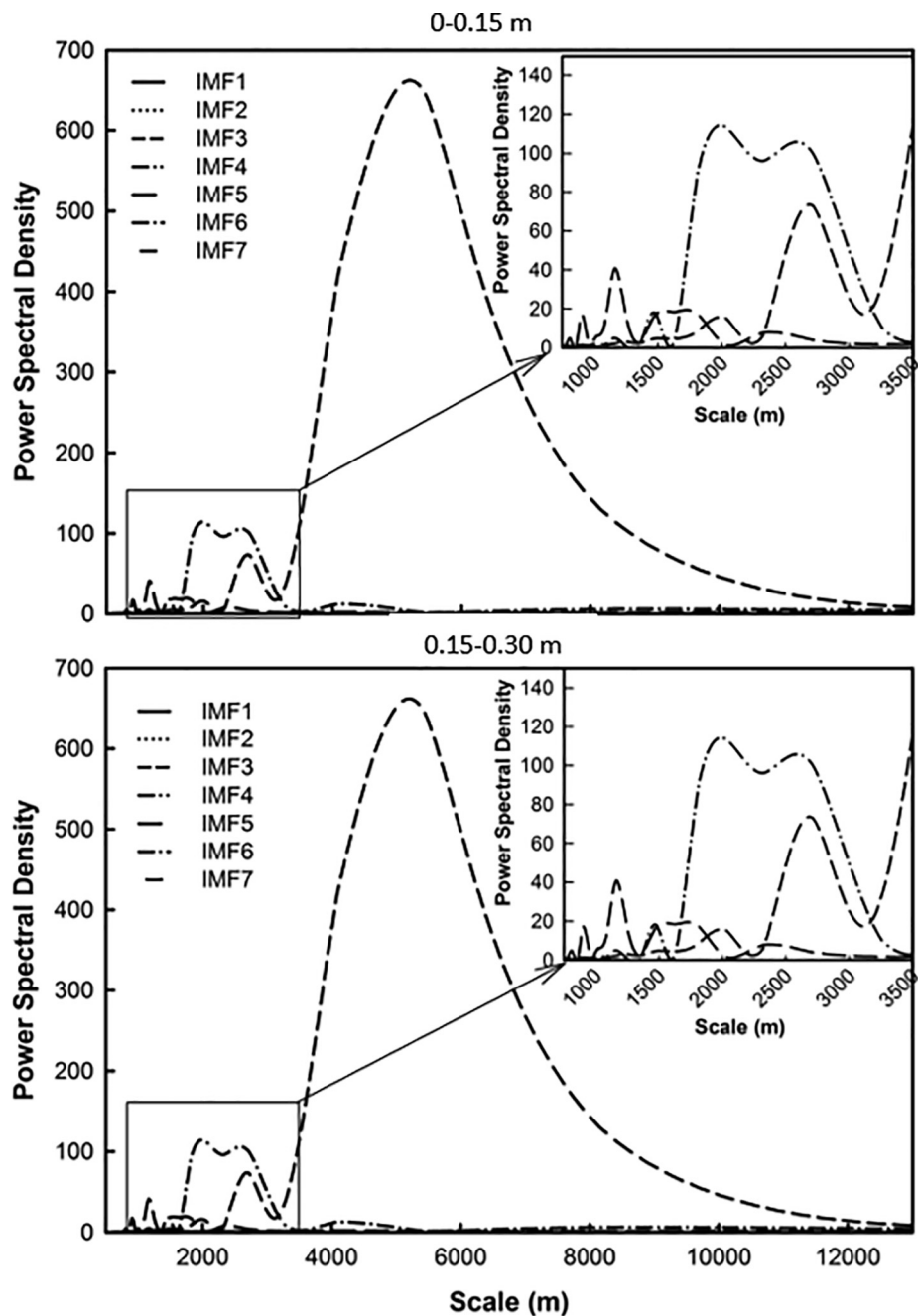


Fig. 4. Scale analysis for the transect 1 two depth intervals.

Table 8
Variation explained by the IMF and residuals for each transect and depth in the spatial series.

Transect	Depth	Variation explained by IMFs	Variation explained by the residual
1	0–0.15 m	60.6	39.4
1	0.15–0.30 m	84.6	15.4
2	0–0.15 m	97.7	2.3
2	0.15–0.30 m	34.6	65.4
3	0–0.15 m	17.6	82.4
3	0.15–0.30 m	10.3	89.7
4	0–0.15 m	91	9
4	0.15–0.30 m	95.6	4.4

acted as a surrogate for climate influences on SOC stocks. For example, MF and most of the SMF vegetation types are located in the wetter south-western slopes of the ranges where average annual rainfall is relatively high (3810–5080 mm, Cooray, 1998). These relatively highly productive, dense, and species rich vegetation types not only results in relatively large inputs of carbon into SOC, but minimises SOC loss from erosion (Bambaradeniya and Ekanayake, 2003; Seely et al., 2010). Also, the MMF vegetation growing in the eastern parts of KFR may have had relatively low SOC stocks when compared to MF and SMF due to the prevailing dry climatic conditions in this region (~2000 mm during the monsoons) (Legg, 1995; Cooray, 1998).

The topography may have also been a surrogate for climate (Post et al., 1982) and soil properties (Wilcox et al., 2002; Prichard et al., 2000). For example, the relatively low temperature due to high elevation of MF and SMF vegetation types may have resulted in relatively slow rates of turnover of SOC, thereby resulting in relatively high SOC

a) Depth 0-0.15 m

b) Depth 0.15-0.30 m

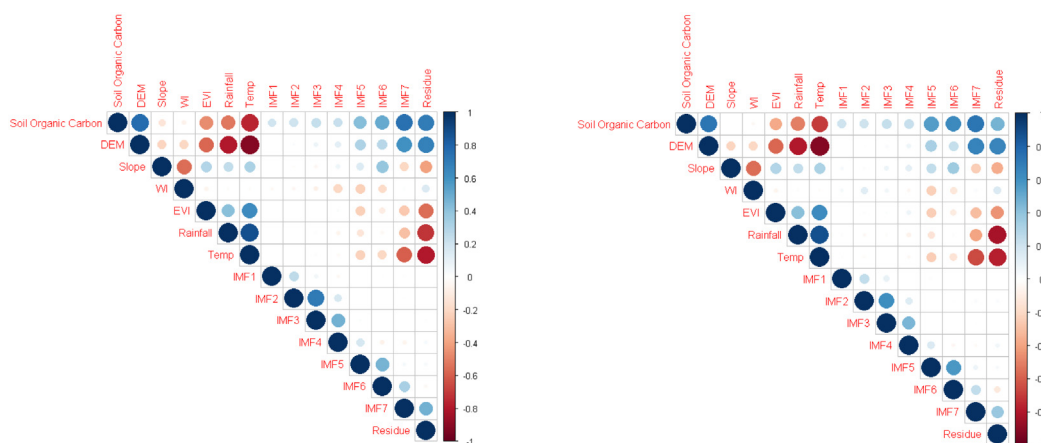


Fig. 5. Correlation analysis for the SOC, environmental covariates, IMFs and residuals for transect 1 of depth interval (a) 0–0.15 m, and (b) 0.15–0.30 m.

Table 9

Soil organic carbon stocks in different vegetation types of Knuckles forest reserve in comparison with estimates of the other forests in the same region.

Landuse types	SOC stock (Mg ha ⁻¹)				Reference
	0–0.15 m	0.15–0.30 m	0–0.30 m	Other	
Montane forests, West Malaysia	26.46	–	–	–	Jeyanny et al. (2014)
Montane forests, Costa Rica	–	–	–	20.5 (0–0.10 m)	Tanner et al. (2016)
Primary forests, Singapore	–	–	–	34.3 (0–0.20 m)	Ngo et al. (2013)
Primary forests, Colombia	–	–	72.18	–	Sierra et al. (2007)
Amazon	–	–	–	23–217 (0–1 m)	Cerri et al. (2000)
Closed canopy forests, Kashmir	33.90	–	–	–	Shaheen et al. (2017)
Evergreen forests, Cambodia	–	–	56.90	–	Toriyama et al. (2011)
Deciduous forests, Cambodia	–	–	34.90	–	Toriyama et al. (2011)
Open forest, Kashmir	28.60	–	–	–	Shaheen et al. (2017)
Disturbed forest, Kashmir	20.60	–	–	–	Shaheen et al. (2017)
Grasslands, Garhwal Himalaya	–	–	75.76	–	Gupta and Sharma (2011)
Sparse shrub/Herbaceous	–	–	43.00	–	Petri et al. (2010)
Pine forests, Garhwal Himalaya	–	–	46.07	–	Gupta and Sharma (2011)
Montane forests	39.10	34.50	–	–	Current study
Sub montane forests	36.00	29.00	–	–	Current study
Moist Monsoon forests	28.00	21.40	–	–	Current study
Open and sparse forests	27.10	23.00	–	–	Current study
Grasslands	27.00	21.10	–	–	Current study
Forest plantations (Pine)	23.90	16.60	–	–	Current study

stocks under these vegetation types (Post et al., 1982; Fissore et al., 2008). Indeed the mean annual temperature could vary between 18.5 and 26 °C in KFR depending on the altitudinal changes (Cooray, 1998).

The anthropogenic activities have already had an influence on SOC (e.g. Larionova et al., 2002). For example, agricultural expansion in the area (tea and chena cultivation), fire and removal of timber from the forest lands have led to the conversion of forests into grasslands over time. Our results demonstrated that the SOC under GL were relatively low when compared to MF and SMF vegetation types, but relatively high when compared to FP vegetation (Table 3). Similarly, OSF vegetation resulted burning forest patches for cultivation purposes. The SOC stocks under this vegetation type were also relatively low probably due to the relatively low input of organic carbon into SOC due to isolated trees scattered over vast expanse of grasslands (Larionova et al., 2002).

It has been reported, higher variation of SOC across the considered transects (Appendix, Fig. A.2). As a result, decomposed SOC signal through EMD analysis to different components of the IMFs and residue resulted different scales (Table 7). The correlation among the IMFs and

continuous environmental covariates exhibited similar pattern (Fig. 5 for transect 1 and Appendix, Fig. A.3 for other transects). While general SOC spatial drivers of the study were identified through spatial LMM, the EMD analysis was able to explore more details about the SOC drivers in KFR. For instance, impact of climatic variables at larger spatial scales can be identified through the EMD analysis which did not reflect in the LMM analysis. The scale specific SOC drivers at different locations may help in identifying the appropriate environmental covariates for detail modelling and mapping of SOC in future applications (Zhou et al., 2016). Additionally, identified scales can be used to determine the sampling interval for detail analysis of SOC with a targeted region in the study region. In current study, the outputs from the spatial LMM analysis were included as inputs to the EMD analysis. Nevertheless, the error propagation from the derived digital SOC maps from the spatial LMM analysis were ignored. This is a limitation of the study and beyond the aims of this manuscript.

As outlined by Sanderman et al. (2011), generally it is recommended to use a correction factor for coarse fragments in the SOC

stock. However, in the current study such correction factor was not included in SOC stock calculations that can lead to errors in the calculated SOC stocks. This is a limitation of the current study. Additionally, having sparse measurement locations across the study region can underestimate the actual variation of SOC stocks in the study region. In the current study, the sampling density was reported as 0.90 per km² ($n = 190$ and area = 210 km²). While this is a bit lower value, for a catchment scale study this value can be considered as acceptable. For example the work carried out by Karunaratne et al. (2014a,b) only recorded sample density of 0.06 per km² ($n = 88$ and area = 1445 km²) for a catchment scale study.

5. Conclusions

Vegetation type (which in turn was partly influenced by climate) was a key factor influencing 0–0.30 m SOC stocks in KFR. Topography also influence 0–0.30 m SOC, the slower turnover of SOC at higher altitudes with relatively low temperatures. Our results also indicated anthropogenic activities influenced SOC, with SOC stocks being relatively low where forests have been fully or partially cleared. This baseline information on SOC stocks will be useful for informing future conservation and management of the KFR considering its highly valuable ecosystem services provided. Additionally, scale specific analysis through EMD provided detail information on influence of SOC drivers at corresponding scales which will be useful in localised modelling of SOC and designing sampling strategies for SOC in future applications.

Declaration of Competing Interest

The authors declare that they have no known competing financial interests or personal relationships that could have appeared to influence the work reported in this paper.

Acknowledgements

Authors are grateful to Mr. A. Pathirana and Ms. Kumuduni Karunaratne for assistance in chemical analysis. Thanks, are also due to Mr. Asanka Pushpakumara for help with soil sampling and sample preparation in the National Institute of Fundamental Studies, Kandy, Sri Lanka. We are thankful to Charitha Adikari Arachchi for her assistance in data analysis and for reading the initial draft of this manuscript.

Appendix A. Supplementary material

Supplementary data to this article can be found online at <https://doi.org/10.1016/j.foreco.2020.118285>.

References

- Albaladejo, J., Ortiz, R., Garcia-Franco, N., Navarro, A.R., Almagro, M., Pintado, J.G., Martinez-Mena, M., 2013. Land use and climate change impacts on SOC stocks in semi-arid Spain. *J. Soil Sediments* 13, 265–277. <https://doi.org/10.1007/s11368-012-0617-7>.
- Assis, C.P., Oliveir, T.S., Dantas, J.A.N., Mendonça, E.S., 2010. Organic matter and phosphorus fractions in irrigated agro ecosystems in a semi-arid region of North Eastern Brazil. *Agric. Ecosyst. Environ.* 138, 74–82. <https://doi.org/10.1016/j.agee.2010.04.002>.
- Baker, K.F., 1976. The determination of organic carbon in soil using a probe-colorimeter. *Lab. Pract.* 25, 82–83.
- Bambaradeniya, C.N.B., Ekanayake, S.P., 2003. A Guide to the Biodiversity of Knuckles Forest Region. IUCN, Colombo, Sri Lanka.
- Benbi, D.K., Brar, K., Toor, A.S., Singh, P., 2015. Total and labile pools of soil organic carbon in cultivated and undisturbed soils in northern India. *Geoderma* 237, 149–158. <https://doi.org/10.1016/j.geoderma.2014.09.002>.
- Biswas, A., Si, B.C., 2011. Revealing the controls of soil water storage at different scales in a hummocky landscape. *Soil Sci. Soc. Am. J.* 75, 1295–1306. <https://doi.org/10.2136/sssaj2010.0131>.
- Biswas, A., Cresswell, H.P., Chau, H.W., Rossel, R.A.V., Si, B.C., 2013. Separating scale-specific soil spatial variability: a comparison of multi-resolution analysis and empirical mode decomposition. *Geoderma* 209, 57–64. <https://doi.org/10.1016/j.geoderma.2013.06.003>.
- Bishop, T.F.A., Horta, A., Karunaratne, S.B., 2015. Validation of digital soil maps at different spatial supports. *Geoderma* 241–242, 238–249. <https://doi.org/10.1016/j.geoderma.2014.11.026>.
- Blake, G.R., Hartge, K.H., 1982. Bulk density. In: Klute, A. (Ed.), *Methods of Soil Analysis*, second ed. American Society of Agronomy Inc., Madison, pp. 374–390.
- Bolton, H., Smith, J.L., Link, S.O., 1993. Soil microbial biomass and activity of a disturbed undisturbed shrub-steppe ecosystem. *Soil Biol. Biochem.* 25, 545–552. [https://doi.org/10.1016/0038-0717\(93\)90192-E](https://doi.org/10.1016/0038-0717(93)90192-E).
- Cambardella, C.A., Moorman, T.B., Parkin, T.B., Karlen, D.L., Novak, J.M., Turco, R.F., Konopka, A.E., 1994. Field-scale variability of soil properties in Central Iowa soils. *Soil Sci. Soc. Am. J.* 58 (5), 1501–1511. <https://doi.org/10.2136/sssaj1994.03615995005800050033x>.
- Cerri, C.C., Bernoux, M., Arrouays, D., Feigl, B.J., Piccolo, M.C., 2000. Carbon stocks in soils of the Brazilian Amazon. In: Lal, R., Kimble, J.M., Stewart, B.A. (Eds.), *Global Climate Change and Tropical Ecosystems*. CRC Press, Florida, pp. 33–50.
- Clark, D.A., 2004. Sources or sinks? The responses of tropical forests to current and future climate and atmospheric composition. *Philos. Trans. R. Soc. Lond. B: Biol. Sci.* 359, 477–491. <https://doi.org/10.1098/rstb.2003.1426>.
- Cooray, P.G., 1998. Knuckles Massif—a portfolio, Forest Department., Forestry Information Service, Sri Lanka.
- De Rosayro, R.A., 1958. The climate and vegetation of the Knuckles region of Ceylon. *Ceylon Forester* 3 (3–4), 201–260.
- Diggle, P.J., Ribeiro Jr., P.J., 2007. *Model Based Geostatistics*. Springer, New York. <https://doi.org/10.1111/1467-9876.00113>.
- Dorji, T., Odeh, I.O., Field, D.J., Baillie, I.C., 2014. Digital soil mapping of soil organic carbon stocks under different land use and land cover types in montane ecosystems, Eastern Himalayas. *For. Ecol. Manage.* 318, 91–102. <https://doi.org/10.1016/j.foreco.2014.01.003>.
- Edmonds, R.L., 1991. Organic matter decomposition in western United States forests. In: Harvey, A.E., Neuenschwander, L.F. (Eds.), *Proceedings-Management and Productivity of Western Montane Forest Soils*. USDA Forest Service General Technical Reports INT 280, pp. 116–128.
- Elliot, W.J., 2003. Soil erosion in forest ecosystems and carbon dynamics. In: Kimble, J.M., Heath, L.S., Birdsey, R.A., Lal, R. (Eds.), *The Potential of US Forest Soils to Sequester Carbon and Mitigate the Greenhouse Effect*, CRC Press (Florida), Chapter 11, pp. 175–190.
- FAO, 2017. GSP Guidelines for sharing national data/information to compile a Global Soil Organic Carbon (GSOC) map. Pillar 4 Working Group, Version 1, Rome.
- Fissore, C., Giardina, C.P., Kolka, R.K., Trettin, C.C., King, G.M., Jurgensen, M.F., Barton, C.D., McDowell, S.D., 2008. Temperature and vegetation effects on soil organic carbon quality along a forested mean annual temperature gradient in North America. *Glob. Change Biol.* 14 (1), 193–205. <https://doi.org/10.1111/j.1365-2486.2007.01478.x>.
- Gupta, M.K., Sharma, S.D., 2011. Sequestered carbon: Organic carbon pool in the soils under different forest covers and land uses in Garhwal Himalayan Region. *Int. J. Agric. Forest.* 1 (1), 14–20. <https://doi.org/10.5923/j.ijaf.2011010103>.
- Hengl, T., de Jesus, J.M., MacMillan, R.A., Batjes, N.H., Heuvelink, G.B., Ribeiro, E., Samuel-Rosa, A., Kempen, B., Leenaars, J.G., Walsh, M.G., Gonzalez, M.R., 2014. SoilGrids1km-global soil information based on automated mapping. *PLoS ONE* 9 (8), e105992. <https://doi.org/10.1371/journal.pone.0105992>.
- Houghton, R.A., 2005. Aboveground forest biomass and the global carbon balance. *Glob. Change Biol.* 11, 945–958. <https://doi.org/10.1111/j.1365-2486.2005.00955.x>.
- Hoyle, F.C., Murphy, D.V., Brookes, P.C., 2008. Microbial response to the addition of glucose in low-fertility soils. *Biol. Fertil. Soils* 44, 571–579. <https://doi.org/10.1007/s00374-007-0237-3>.
- Huang, Norden E., Shen, Zheng, Long, Steven R., Wu, Manli C., Shih, Hsing H., Zheng, Qunan, Yen, Nai-Chyuan, Tung, Chi Chao, Liu, Henry H., 1998. The empirical mode decomposition and the Hilbert spectrum for nonlinear and non-stationary time series analysis. *Proc. R. Soc. Lond. A* 454 (1971), 903–995. <https://doi.org/10.1098/rspa.1998.0193>.
- Huang, J., Shi, Z., Biswas, A., 2015. Characterizing anisotropic scale-specific variations in soil salinity from a reclaimed marshland in China. *Catena* 131, 64–73. <https://doi.org/10.1016/j.catena.2015.03.011>.
- IUSS Working Group WRB, 2015. World Reference Base for Soil Resources 2014, update 2015 International soil classification system for naming soils and creating legends for soil maps. World Soil Resources Reports No. 106. FAO, Rome.
- Jandl, R., Lindner, M., Vesterdal, L., Bauwens, B., Baritz, R., Hagedorn, F., Johnson, D.W., Minkinen, K., Byrne, K.A., 2007. How strongly can forest management influence soil carbon sequestration? *Geoderma* 137 (3–4), 253–268.
- Jenny, H., 1994. *Factors of Soil Formation: A System of Quantitative Pedology*. Dover Publications, INC, New York.
- Jeyanny, V., Husni, M.H.A., Rasidah, K.W., Kumar, B.S., Arifin, A., Hisham, M.K., 2014. Carbon stocks in different carbon pools of a tropical lowland forest and a montane forest with varying topography. *J. Trop. For. Sci.* 560–571. <https://www.jstor.org/stable/43150942>.
- Karunaratne, S.B., Bishop, T.F.A., Baldock, J.A., Odeh, I.O.A., 2014a. Catchment scale mapping of measurable soil organic carbon fractions. *Geoderma* 219, 14–23. <https://doi.org/10.1016/j.geoderma.2013.12.005>.
- Karunaratne, S.B., Bishop, T.F.A., Odeh, I.O.A., Baldock, J.A., Marchant, B.P., 2014b. Estimating change in soil organic carbon using legacy data as the baseline: issues, approaches and lessons to learn. *Soil Res.* 52, 349–365. <https://doi.org/10.1071/SR13081>.
- Kölbl, A., Schad, P., Jahn, R., Amelung, W., Bannert, A., Cao, Z.H., Fiedler, S., Kalbitz, K., Lehndorff, E., Müller-Niggemann, C., Schloter, M., Schwark, L., Vogelsang, V., Wissing, L., Kögel-Knabner, I., 2014. Accelerated soil formation due to paddy

- management on marshlands (Zhejiang Province, China). *Geoderma* 228, 67–89. <https://doi.org/10.1016/j.geoderma.2013.09.005>.
- Lal, R., 2005. Forest soils and carbon sequestration. *For. Ecol. Manage.* 220 (1–3), 242–258.
- Lal, R., 2015. Restoring soil quality to mitigate soil degradation. *Sustainability* 7 (5), 5875–5895.
- Lark, R.M., Cullis, B.R., Welham, S.J., 2006. On spatial prediction of soil properties in the presence of a spatial trend: the empirical best linear unbiased predictor (E-BLUP) with REML. *Eur. J. Soil Sci.* 57 (6), 787–799. <https://doi.org/10.1111/j.1365-2389.2005.00768.x>.
- Larionova, A.A., Rozanova, L.N., Evdokimov, I.V., Ermolaev, A.M., 2002. Carbon budget in natural and anthropogenic forest-steppe ecosystems. *Pochvovedenie* 2, 177–185.
- Legg, C., 1995. A Geographic information system for planning and managing the Conservation of tropical forest in the Knuckles Range. *The Sri Lanka Forester* 25–36.
- McBratney, A.B., Field, D.J., Koch, A., 2014. The dimensions of soil security. *Geoderma* 213, 203–213. <https://doi.org/10.1016/j.geoderma.2013.08.013>.
- McBratney, A.B., Santos, M.L.M., Minasny, B., 2003. On digital soil mapping. *Geoderma* 117 (1–2), 3–52. [https://doi.org/10.1016/S0016-7061\(03\)00223-4](https://doi.org/10.1016/S0016-7061(03)00223-4).
- Mishra, U., Lal, R., Slater, B., Calhoun, F., Liu, D., Van Meirvenne, M., 2009. Predicting soil organic carbon stock using profile depth distribution functions and ordinary kriging. *Soil Sci. Soc. Am. J.* 73 (2), 614–621. <https://doi.org/10.2136/sssaj2007.0410>.
- Ngo, K.M., Turner, B.L., Muller-Landau, H.C., Davies, S.J., Larjavaara, M., Bin Nik Hassan, N.F., Lum, S., 2013. Carbon stocks in primary and secondary tropical forests in Singapore. *For. Ecol. Manage.* 296, 81–89. <https://doi.org/10.1016/j.foreco.2013.02.004>.
- Ottoy, S., De Vos, B., Sindayihebura, A., Hermy, M., Van Orshoven, J., 2017. Assessing soil organic carbon stocks under current and potential forest cover using digital soil mapping and spatial generalisation. *Ecol. Ind.* 77, 139–150. <https://doi.org/10.1016/j.ecolind.2017.02.010>.
- Overby, S.T., Hart, S.C., Neary, D.G., 2003. Impacts of natural disturbance on soil carbon dynamics in forest ecosystems. In: Kimble, J.M., Heath, L.S., Birdsey, R.A., Lal, R. (Eds.), *The Potential of US Forest Soils to Sequester Carbon and Mitigate the Greenhouse Effect*. CRC Press (Florida), Chapter 10, 159–172.
- Panabokke, C.R., 1996. Soils and agro-ecological environments of Sri Lanka. NARESA.
- Pebesma, E.J., 2004. Multivariable geostatistics in S: the gstat package. *Comput. Geosci.* 30, 683–691. <https://doi.org/10.1016/j.cageo.2004.03.012>.
- Petri, M., Batello, C., Villani, R., Nachtergaele, F., 2010. Carbon status and carbon sequestration potential in the world's grasslands. *Grassland Carbon Sequestr.: Manage., Policy Econ.* 11, 19.
- Pinheiro, J., Bates, D., DebRoy, S., Sarkar, D., R Core Team, 2019. nlme: Linear and Nonlinear Mixed Effects Models. R package version 3.1-142.
- Post, W.M., Emanuel, W.R., Zinke, P.J., Stangenberger, A.G., 1982. Soil carbon pool and world life zones. *Nature* 298 (5870), 156–159. <https://doi.org/10.1038/298156a0>.
- Prichard, S.J., Peterson, D.L., Hammer, R.D., 2000. Carbon distribution in subalpine forests and meadows of the Olympic Mountains, Washington. *Soil Sci. Soc. Am. J.* 64 (5), 1834–1845.
- Ratnayake, R.R., Karunaratne, S.B., Lessels, J.S., Yogenthiran, N., Rajapaksha, R.P.S.K., Gnanavelrajah, N., 2016. Digital soil mapping of organic carbon concentration in paddy growing soils of Northern Sri Lanka. *Geoderma Regional* 7, 167–176. <https://doi.org/10.1016/j.geodrs.2016.03.002>.
- Ratnayake, R.R., Perera, B.M.A.C.A., Rajapaksha, R.P.S.K., Ekanayake, E.M.H.G.S., Kumara, R.K.G.K., Gunaratne, H.M.A.C., 2017. Soil carbon sequestration and nutrient status of tropical rice based cropping systems: rice-rice, rice-soya, rice-onion and rice-tobacco in Sri Lanka. *Catena* 150, 17–23. <https://doi.org/10.1016/j.catena.2016.11.006>.
- Sanderman, J., Baldock, J., Hawke, B., Macdonald, L., Massis-Puccini, A., Szarvas, S., 2011. National soil carbon research programme: field and laboratory methodologies. CSIRO Land and Water, Waite Campus, Urrbrae SA 5064, Australia.
- Scheller, R.M., Hua, D., Bolstad, P.V., Birdsey, R.A., Mladenoff, D.J., 2011. The effects of forest harvest intensity in combination with wind disturbance on carbon dynamics in Lake States Mesic Forests. *Ecol. Model.* 222 (1), 144–153.
- Seely, B., Welham, C., Blanco, J.A., 2010. Towards the application of soil organic matter as an indicator of forest ecosystem productivity: deriving thresholds, developing monitoring systems, and evaluating practices. *Ecol. Ind.* 10, 999–1008. <https://doi.org/10.1016/j.ecolind.2010.02.008>.
- Shaheen, H., Saeed, Y., Abbasi, M.K., Khaliq, A., 2017. Soil carbon stocks along an altitudinal gradient in different land-use categories in Lesser Himalayan foothills of Kashmir. *Eurasian Soil Sci.* 50 (4), 432–437. <https://doi.org/10.1134/S106422931704010X>.
- Sierra, C.A., Del Valle, J.I., Orrego, S.A., Moreno, F.H., Harmon, M.E., Zapata, M., Colorado, G.J., Herrera, M.A., Lara, W., Restrepo, D.E., 2007. Total carbon stocks in a tropical forest landscape of the Porc region, Colombia. *For. Ecol. Manage.* 243 (2–3), 299–309. <https://doi.org/10.1016/j.foreco.2007.03.026>.
- Sousa, F.P., Ferreira, T.O., Mendonça, E.S., Romero, R.E., Oliveira, J.G.B., 2012. Carbon and nitrogen in degraded Brazilian semi-arid soils undergoing desertification. *Agric. Ecosyst. Environ.* 148, 11–21. <https://doi.org/10.1016/j.agee.2011.11.009>.
- Stockmann, U., Adams, M.A., Crawford, J.W., Field, D.J., Henakarchchi, N., Jenkins, M., Minasny, B., McBratney, A.B., De Courcelles, V.D.R., Singh, K., Wheeler, I., 2013. The knowns, known unknowns and unknowns of sequestration of soil organic carbon. *Agric. Ecosyst. Environ.* 164, 80–99. <https://doi.org/10.1016/j.agee.2012.10.001>.
- Stockmann, U., Padarian, J., McBratney, A., Minasny, B., de Brogniez, D., Montanarella, L., Hong, S.Y., Rawlins, B.G., Field, D.J., 2015. Global soil organic carbon assessment. *Global Food Security* 6, 9–16. <https://doi.org/10.1016/j.gfs.2015.07.001>.
- Tanner, L.H., Wilckens, M.T., Nivison, M.A., Johnson, K.M., 2016. Biomass and soil carbon stocks in Wet Montane Forest, Monteverde Region, Costa Rica: assessments and challenges for quantifying accumulation rates. *Int. J. Forestry Res.* 2016. <https://doi.org/10.1155/2016/5812043>.
- Toriyama, J., Ohnuki, Y., Eriko, I.T.O., Kanzaki, M., Araki, M., Chann, S., Bora, T.I.T.H., Samkol, K.E.T.H., Hirai, K., Kiyono, Y., 2011. Soil carbon stock in cambodian monsoon forests. *Japan Agric. Res. Quart.: JARQ* 45 (3), 309–316. <https://doi.org/10.6090/jarq.45.309>.
- Viscarra Rossel, R.A., Webster, R., Bui, E.N., Baldock, J.A., 2014. Baseline map of organic carbon in Australian soil to support national carbon accounting and monitoring under climate change. *Glob. Change Biol.* 20 (9), 2953–2970. <https://doi.org/10.1111/gcb.12569>.
- Werner, W.L., 1982. The upper montane rain forest of Sri Lanka. *The Sri Lanka Forester* 15 (3–4), 119–129.
- Wilcox, C.S., Dominguez, J., Parmelee, R.W., McCartney, D.A., 2002. Soil carbon and nitrogen dynamics in *Lumbricus terrestris*. L. middens in four arable, a pasture, and a forest ecosystems. *Biol. Fertil. Soils* 36 (1), 26–34. <https://doi.org/10.1007/s00374-002-0497-x>.
- Xia, X., Yang, Z., Liao, Y., Cui, Y., Li, Y., 2010. Temporal variation of soil carbon stock and its controlling factors over the last two decades on the southern Song-nen Plain, Heilongjiang Province. *Geosci. Front.* 1, 125–132. <https://doi.org/10.11821/yj2007060002>.
- Zhou, Y., Biswas, A., Ma, Z., Lu, Y., Chen, Q., Shi, Z., 2016. Revealing the scale-specific controls of soil organic matter at large scale in Northeast and North China plain. *Geoderma* 271, 71–79. <https://doi.org/10.1016/j.geoderma.2016.02.006>.
- Zhu, M., Feng, Q., Qin, Y., Cao, J., Li, H., Zhao, Y., 2017. Soil organic carbon as functions of slope aspects and soil depths in a semiarid alpine region of Northwest China. *Catena* 152, 94–102. <https://doi.org/10.1016/j.catena.2017.01.011>.